11-2007

Assessment of Human Trabecular Architecture in the Pubis by Three Radiographic Modalities

Andrew D. Wade
The University of Western Ontario, awade4@uwo.ca

Andrew J. Nelson
The University of Western Ontario, anelson@uwo.ca

Gregory J. Garvin
The University of Western Ontario, ggarvin@sympatico.ca

David W. Holdsworth
The University of Western Ontario, dholdsworth@robarts.ca

Assessment of human trabecular architecture in the pubis by three radiographic modalities

Andrew D Wade[1], Andrew J Nelson[1], Gregory J Garvin[2], David W Holdsworth[3]

Department of [1]Anthropology and [3]Schulich School of Medicine and Dentistry, University of Western Ontario & [2]St.Joseph's Health Care, London

Introduction

This poster discusses technical aspects of an investigation into the use of non-destructive radiological analyses of pubic cancellous bone structure to estimate age-at-death from human skeletal remains. This study stems from findings, in X-ray plain films, of increased rarification and orientation of trabeculae with age [1]; likely in concert with the macroscopic remodelling of the symphyseal surface currently used in estimation of age-at-death.

The study uses three non-destructive X-ray imaging modalities: plain film radiography, computed tomography (CT), and micro-CT (µCT). Plain film radiography has greater spatial resolution than CT [2] and is relatively inexpensive, widely available, and, with portable X-ray units, even accessible in the field for archaeological and forensic applications. CT scanners are largely restricted to clinical settings due to the size, sensitivity, and cost of the machine, but offer a greater contrast resolution than plain film radiography [2]. More expensive and more precise, µCT scanners are further restricted in their availability and accessibility, but CT and µCT modalities provide volumetric data, avoiding the confusion of overlying cortical and cancellous structures and the apparent increases in density with element thickness seen in plain film radiography.

1. Plain Film Radiography

a) Data Acquisition

The pelves were X-rayed (60 kV, 0.2 mA, 2 min.) in the antero-posterior view, using Kodak Ektavision 5 film.

No intensifying screen used

- Spatial resolution without a screen is almost perfect [2]
- Longer exposure time necessary
- Patient radiation dose was not a risk factor

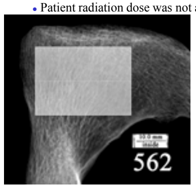

Figure 1. ROI defined in plain film radiograph

Rectangular region of interest (ROI) marked at right angles to the symphyseal surface.

- One side immediately beneath symphyseal surface
- Encompassing as much cancellous bone as possible
- No cortical bone included
- Horizontal ROI midline marker added to register midline measurements

1b) Data Processing

Scanned plain films were marked with a scale, to calibrate the software measurements, and an ROI and imported to the Image Pro Express software for analysis.

Line profile tool - measuring changes in pixel value along a line

- Used to measure the intensity of the imaged trabecular structures
- Along three lines in the ROI parallel to the symphyseal surface
  - running supero-inferior
  - immediately above mid-line and inside upper and lower bounds

Thick horizontal profile tool - measures mean over designated area

- Upper and a lower area profile were measured
- Average of the two used for the total area mean.

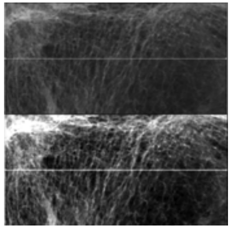

Figure 2. Regular (above) and high contrast images of a scanned plain film

It was initially believed that a count of the peaks on graphs of the line profiles would provide an accurate count of the trabeculae crossing that line for the purpose of determining the linear trabecular density (intersections per mm). The peak counts were compared to three consecutive direct visual counts using a high contrast image and found to be significantly different ($p<0.02$). For this reason, the averages of three consecutive visual counts, to mitigate intra-observer error, were used to calculate linear trabecular densities rather than the profile peak counts.

Values of Interest

- Upper and lower area pixel value means
  - used to calculate total area mean
- Upper, lower, and middle linear pixel value means
- Height and width of the ROI
- Upper, lower, and middle linear counts of trabeculae
  - used to calculate a linear trabecular density using the ROI width

2. Computed Tomography

a) Data Acquisition

The dry bone pelves were scanned in a GE Lightspeed Volumetric CT scanner at a slice thickness of 0.625 mm. Clinical scanning protocols and reconstruction algorithms provided poor resolution of the trabeculae

- Bettered slightly by surrounding the sample with lactated ringers
- Due to artifacts caused by the direct air to bone interface

Clinical CT scanners are finely calibrated for use on living patients and artefacts are believed to have occurred, increasing image noise, due to the significantly different beam hardening [3] that results when dry bone alone is scanned.

Scans, where samples were embedded in gelatin (see Jello, center), were found to have visibly improved resolution of trabecular structure.

- Scanned individually in a tray made of construction foam
  - radio-density of foam is extremely low
- Tray filled with gelatin
- Ilium on foam wedges to keep the AP plane parallel to scanner bed
  - medial end of pubis faces scanning gantry (Z-axis medio-lateral)

Each pubis was scanned as follows:

- Scout Scan – to locate an ROI encompassing the pubis
- Standard Axial Scan – 0.625 mm thickness, 120 kV, 200 mA, 0 pitch
- Recon Scan – edge reconstruction algorithm applied to standard scan

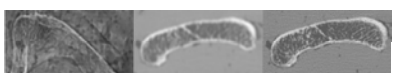

Figure 3. Scout, standard axial, and edge recon CT scans

Jello

In order to improve the resolution of trabecular structures in CT scans, a protocol was devised for simulating soft-tissue in close contact with the sample. While water is the ideal medium for simulating soft-tissue, the scientific value of the sample precluded immersion.

Jello Brand Gelatin

- Radio-density similar to water
- Not fluid enough to flow into protective wrappings
- Fluid enough to conform to the shape of the sample
- Used in radiology of urinary calculi (as calibration phantom)[4]

Glad Press'n Seal Adhesive Wrap

- Adheres to bone to produce minimal air space
- Does not adhere enough to damage the bone's surface

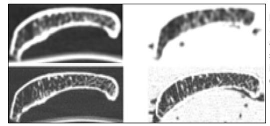

Figure 4. Standard (above) and edge recon scans of samples in air (left) and gelatin

HMH Thresholding

When bone and air are found in the same voxel (3D pixel), the resulting radio-density value for that voxel is an averaged value (partial volume effect). As such, a threshold value must be provided above which all material is treated as bone and below as non-bone. Differences in threshold can lead to over- or under-representation of trabecular structures.

To ensure repeatability and objectivity the half-maximum height (HMH) thresholding method was chosen over the visual method of thresholding; that is, adjusting the threshold manually for perceived trabecular connection and shape.

Thresholding Method

- Adapted from Fajardo and colleagues [5]
- Uses histogram of the radio-densities for a small region of the scan that includes a trabecular bone-air interface
- Maximum value recorded for 10 random interfaces
- Average of one-half max value is the regional threshold

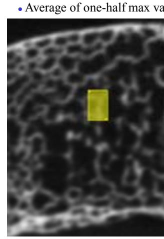

Figure 5. Selection of a bone-air interface for HMH thresholding in a micro-CT scan

The µCT data ranged from approx. -1000 HU (air) to +3095 HU (metal pins) and were treated differently

- Established HMH method uses average of min and max values
- Too much variation was found in minimum values
  - partial volume effect in tiny inter-trabecular spaces
  - expected to represent only air
- Standard value for air (-1000 HU) was used as the minimum value for the HMH calculations on 10 random trabeculae in the µCT scan.

2b) Data Processing

DICOM (Digital Imaging and COmmunications in Medicine) scan slices were imported to the Microview CT/µCT analysis software and reconstructions of the volumes created.

Volume of interest (VOI) designated with

- One side behind the symphyseal surface
- Encompassing as much cancellous bone as possible
- No cortical bone included

A local threshold for the VOI was determined, using the half-maximum height (HMH) thresholding method (see HMH, center), and stereology information was calculated by Microview

Values of Interest

- Bone and tissue volumes
- Trabecular thickness and separation
- Trabecular number – density measure
- Connectivity density

The ratio of bone to tissue (total) volume of the VOI is a measure of the overall bone density and the ratio of bone surface to volume is used in calculations of trabecular thickness [6].

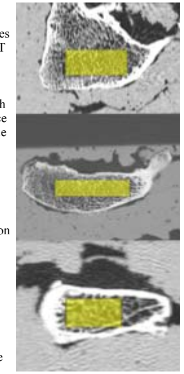

Figure 6. VOI defined in (top to bottom) AP, SI, and ML planes of a CT reconstruction

The slice thickness (0.625 mm) is substantially greater than the spatial resolution within the slices (0.248 mm to 0.293 mm), resulting in loss of information about

- Actual connectivity
- Medio-lateral organization of cancellous bone
- Anisotropy - tendency to orient in a particular direction
  - all transversely anisotropic in the Z-axis (ML) regardless of the actual trabecular architecture (confirmed against near isotropic µCT scans)

3. Micro-CT

a) Data Acquisition

The pelves were scanned in a GE Locus Ultra 150µm µCT scanner (120 kV, 20.0 mA, 16.0 s). Due to the restrictive size of both the scanner gantry (240 mm diameter) and the scanner's optimal field of view (120 mm diameter), the pelves were oriented with the symphyseal surface facing down into the scanner bed.

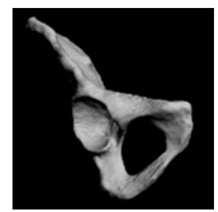

Figure 7. 3D pelvis reconstruction

Orientations were adjusted according to the fit of individual pelves

- Ensures pubis is as close to the center of the optimal field of view
- Isotropic nature of the µCT voxels allows for re-orientation
  - minimal loss of information
- All reconstructions placed in same orientation as CT reconstructions
  - oriented for comparable analysis

3b) Data Processing

The µCT reconstructions were imported to the Microview CT/µCT analysis software and re-oriented to match the CT reconstructions.

- µCT VFF files increase in size with re-orientation
- Files often exceed the size restriction of the software, therefore
  - Reconstructions were first cropped to remove all but the pubis
    - to the midline of the obturator foramen.
  - Cropped reconstructions then re-oriented
    - X-axis was SI, the Y-axis was AP, and the Z-axis was ML
  - Further cropped to reduce loading and processing times

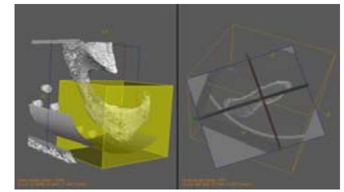

Figure 8. Cropping (left) and re-orientation (right) processes

In each pubis a volume of interest (VOI) was designated in the same manner as in the CT reconstructions. A local threshold for the VOI was determined using a modified HMH thresholding method (see HMH, center), and the stereology information was calculated by the Microview program. Values of interest include, in addition to the CT values, anisotropy (the tendency of structures to orient in a particular direction) and connectivity density.

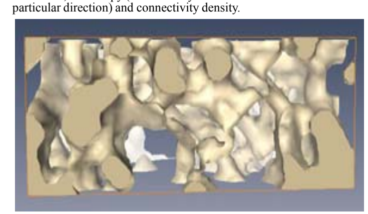

Figure 9. 3D reconstruction of a region of cancellous bone from a micro-CT scan

Conclusion

Radiographic methods provide an additional line of evidence in age estimation along with a non-destructive option for assessment, digital preservation, and electronic sharing of remains that are either incompatible with macroscopic techniques (i.e. fragmentary remains, wrapped mummies) or culturally-sensitive archaeological and forensic materials which must remain unmodified for future researchers or for repatriation and reburial. The three radiographic imaging methods presented here provide varying degrees of spatial and contrast resolution at different levels of expense and availability. Analysis of the relation of the measures here to age-at-death is ongoing, with the goal of producing Bayesian predictive models. Preliminary analysis suggests all three modalities have predictive power, with greater error at decreasing resolutions. Judicious use of any and all of these methods, applied to the question of age-at death, provides the researcher with an alternative to the traditional macroscopic examination and destructive, two-dimensional thin section microscopy.

Literature cited

[1] DeLaurier A. 1998. The effects of habitual biochemical stress, trauma and pathology on the development and age-related degeneration of the male pubic symphysis. MA Thesis. University of Western Ontario.

[2] Bushberg JT, Seibert AJ, Leidholt EM Jr., and Boone JM. 2002. The essential physics of medical imaging: second edition. New York: Lippincott Williams & Williams

[3] Spoor CF, Jeffery N, and Zonneveld FW. 2000. Imaging skeletal growth and evolution. In: O'Higgins P & Cohn MJ, editors. Development, growth, and evolution: implications for the study of the hominid skeleton. San Diego: Academic Press, p.123-161

[4] Mostafavi MR, Ernst RD, and Saltzman B. 1998. Accurate determination of chemical composition of urinary calculi by spiral computerized tomography. The Journal of Urology 159(3):673-675

[5]Fajardo RJ, Ryan TM, and Kappelman J. 2002. Assessing the accuracy of high-resolution X-ray computed tomography of primate trabecular bone by comparisons with histological sections. American Journal of Physical Anthropology 118:1-10

[6] Borah B, Gross GJ, Dufresne TE, Smith TS, Cockman MD, Chmielewski PA, Lundy MW, Hartke JR, and Sod EW. 2001. Three-dimensional microimaging (MRmicroI and microCT), finite element modelling, and rapid prototyping provide unique insights into bone architecture in osteoporosis. The Anatomical Record (Part B: The New Anatomist) 265:101-110

Acknowledgments

Scanning time was donated by St. Joseph's Healthcare, London (CT) and by the Robarts Research Institute (micro-CT). We thank Karen Betteridge and Rosemary Miller at St.Joseph's and Joseph Umoh at Robarts for technical assistance. Skeletal samples were provided by the Grant Skeletal Collection and the Dakhleh Oasis Project. Funding for this project was provided by the Ontario Graduate Scholarship and the Faculty Scholar Grant to Andrew Nelson.

For further information

Please contact *awade4@uwo.ca*.
Andrew Wade
c/o Department of Anthropology,
Social Science Centre
University of Western Ontario,
London, ON, N6A 5C2